Highlights

- A new magnetic graphene oxide was synthesized, characterized and tested as a sorbent.
- This sorbent was used in a magnetic solid phase extraction on line ICP OES method.
- A simultaneous determination of 8 elements (noble metals, Sb, Hg) has been addressed.
- The method is totally automatic and has been applied to the analysis of sea waters.
- This is the first MSPE method online that uses functionalized MGO as an adsorbent.

Simultaneous determination of noble metals, Sb and Hg by magnetic solid phase extraction on line ICP OES based on a new functionalized magnetic graphene oxide

J.C. García-Mesa, P. Montoro Leal, M.M. López Guerrero*, E.I. Vereda Alonso*

Department of Analytical Chemistry, Faculty of Sciences, University of Malaga, Campus of Teatinos, 29071 Málaga, Spain

Abstract

The aim of this study is to evaluate the extraction capacity of a new functionalized magnetic graphene oxide (MGO) to be employed in the automatic simultaneous preconcentration-determination of a relatively large number of elements with different properties by inductively coupled plasma optical emission spectrometry (ICP OES). A multimode sample introduction system (MSIS) cyclonic spray chamber was employed to generate and introduce vapours of Ag, Au, Ir, Os, Pd, Pt, Sb and Hg in the ICP torch. Several flow and chemical variables were optimized by two multivariate central composite designs. Detection limits between 0.05 μg L^{-1} for Hg, and 2.6 μg L^{-1} for Pd, and enrichment factors between 3 for Hg, and 33 for Os were obtained with a precision ≤5% (%RSD). The accuracy of the method was validated by determining the eight target elements in a certified reference material TMDA 54.5 and by the analysis of spiked tap water, mineral water and sea water samples taken from Málaga (Spain). The obtained results were in good agreement with the certified values and high recoveries were achieved for the spiked samples. Thus, the new adsorbent has demonstrated to be useful for the preconcentration of elements with quite different properties, such as noble metals, Sb and Hg, with a sample throughput of about 13 h^{-1} and low consumption of reagents and samples.

Keywords*:* ICP OES; magnetic solid phase extraction; magnetic graphene oxide; PGMs; antimony; mercury;

*Corresponding authors

E-mail address: mmlopez@uma.es (M.M. López Guerrero); eivereda@uma.es (E.I. Vereda Alonso)

1. Introduction

Graphene oxide (GO) is a novel two-dimensional carbon-based nanomaterial (a single layer of sp^2 bonded carbon atoms in a two-dimensional hexagonal lattice), possessing oxygen-containing groups and large surface area which makes it ideal for retention of analytes compared to carbon nanotubes or even graphene [1-3]. These oxygen-containing groups may serve as binding sites for metal ions. However, un-functionalized GO have not enough selectivity for efficient retention of metals because the oxygen-containing functional groups provide weak coordination with metals ions. In order to further improve selectivity and adsorption properties, various graphene-based nanocomposites have been synthesized by chemical modification of GO [4-7]. Furthermore, it is difficult to separate graphene or GO from aqueous solution using traditional centrifugation and filtration method due to its small particle size. To solve this problem, magnetic nanoparticles (MNPs) can be dispersed on the graphene oxide sheets and quickly extracted by a magnetic field, without the need to filter or centrifuge. MNPs also offer a high surface area, besides of a short diffusion route, producing high extraction efficiency (high extraction capacity with rapid dynamics). Moreover, the surface of MNPs can be readily modified with organic functional groups to obtain selective extraction. However, MNPs can easily form large aggregates, which could decrease the specific surface area and alter their magnetic properties [8-9].The coupling between MNPs and GO seeks compensation for the disadvantages of both materials, favouring the dispersion over GO layers, and so, avoiding the agglomeration of MNPs, besides the need to filter or centrifuge in order to separate the sorbent. Obviously, the union of both adsorbents would even result in a better one. To the best of our knowledge, the use of magnetic graphene oxide (MGO) as

adsorbent in magnetic solid phase extraction (MSPE) is quite recent, 2012 [10], and was first employed towards the preconcentration of organic compounds due to its large delocalized π-electron system, which permits form a strong π–π stacking interaction with compounds with benzene rings [10-12], also MGO has been used for enhanced cleanup procedures in order to eliminate matrix effects before analysis of organic compounds by LC-MS/MS [13,14]. Due to its weak coordination with metals ions, MGO had to be functionalized to be employed in the MSPE of metal ions [15-22]. Although, its applications as extractant in MSPE have always been in batch procedures. This type of procedure requires large sample volumes, shows low sampling frequencies and can suffer analyte losses. The on-line SPE mode shows better sensitivity and reproducibility, reduces sample manipulation and sample preparation time, allows full automation of the system, lower detection limits and minimizes errors [23].

CVG atomic spectrometry is currently the most popular technique for the routine determination of trace amounts of elements which generate volatile species, because of the enhanced detection limits attained in comparison with conventional nebulization of a sample [24]. However, the technique is applicable to a few elements and thus cannot be considered as a general solution to improve sensitivity. To solve this inconvenience McLaughlin and Brindle described the Multimode Sample Introduction System (MSIS) designed for ICP OES [25]. MSIS combines both nebulization and chemical vapour generation (CVG), providing lower detection limits for a number of elements that form volatile species through the reaction with $NaBH_4$ and improving precision without sacrificing the sensitivity.

Platinum group metals (PGMs) are employed in numerous technological applications and, at the same time, they are not found in large concentrations in the natural

environment, being faced with the limit of exploitation of these natural resources. The available information regarding PGMs emissions, environmental concentrations and related toxicity are discussed in several review papers [26,27]. Furthermore, precious metal elements such as Ag, Au, Pt, and Pd are among the rarest elements in the crust [28], where it is most commonly found in high concentrations in areas of ore mineralization. Recently, research regarding the distribution of precious metallic elements has been increased, in particular, to understand the effect of these elements on the environment, and also to aid in their recovery for economic purposes [29]. PGMs, and other elements like Sb are among the raw materials marked as "critical" by the European Union in 2017, meaning raw materials with a high supply-risk and a high economic importance to which reliable and unhindered access is a concern for European industry and value chains [30]. On the other hand, Sb element is potentially toxic even at low concentration and has no biological function [31]. Sb is a metalloid element with potential toxicity and carcinogenicity, and it is widespread in the environment [32]. And, mercury (Hg) has received special attention because of its potential to cause adverse effects on human health and the environment throughout the world. Mercury, a worldwide pollutant from natural or anthropogenic sources, can be globally transported and released to the environment [33].

Due to the fact the monitoring and control of these trace elements in the environment and in food sources require processing a large number of samples to accurately characterize their abundance and to reach reliable conclusions, so automatic, fast and simple methods are necessary. In this work, a new functionalized MGO, 1,5-bis(di-2-pyridil) methylene thiocarbonhydrazide, chemically linked to iron oxide MNPs and GO (DPTH@MGO) has been

fabricated and characterized. From the study of its adsorption capacity towards noble and heavy metals, a new on line automatic method for the simultaneous preconcentration and determination of trace amounts of Ag, Au, Ir, Os, Pd, Pt, Sb and Hg by CVG inductively coupled plasma optical emission spectrometry (ICP OES) has been optimized and applied to environmental water samples. The developed method was validated by determining the eight target elements in a certified reference material TMDA 54.5 and by the analysis of spiked tap water, mineral water and sea water samples (containing high percentages of dissolved salts) gathered from Málaga (Spain).

2. Experimental

2.1. Instrumentation

An inductively coupled plasma optical emission spectrometer, Perkin Elmer Optima 7300 DV (Concord, Canada) implemented with a Marathon Scientific Multimode Sample Introduction System cyclonic spray chamber (MSIS) (Ontario, Canada) and a Perkin Elmer AS-91 autosampler (Concord, Canada) connected with a Perkin Elmer FIAS 400 AS system (Concord, Canada) was used throughout. The FIAS manifold was connected directly with the ICP and was controlled by Optima software. In Table 1 the optimum operation conditions were showed. The selected analytical lines were: Ag 338.289 nm, Au 267.595 nm, Ir 224.268 nm, Os 228.226 nm, Pt 214.423 nm, Pd 340.458 nm, Sb 206.836 nm and Hg 253.652 nm.

50 mg of DPTH@MGO was packed in a PTFE tube (150 mm x 0.5 mm i.d.) which was knotted round a Nd/Fe/B toroidal magnet (2 tesla, 81.4 N holding strength) and placed between other two identical Nd/Fe/B magnets. This reactor was located in the five-port rotatory valve of the FIAS 400 system. Two Omnifit

polyethylene frits (Cambridge, UK) were fixed at both ends of the knotted reactor (KR) to prevent material losses. To deliver the samples, reagents and wastes were used PVC pump tubings. The FIAS 400 system was coupled and operated completely synchronously with the ICP OES.

A Perkin Elmer Spectrum 100 FTIR spectrometer (Concord, Canada) was used to record IR Spectra. The samples were measured as potassium bromide pellets at 1% (wt/wt) approximately.

A Physical Electronics PHI 5700 instrument (Eden Prairie, MN, USA) with a Mg Kα X-ray excitation source (hν=1253.6 eV) was employed for XPS analysis; binding energies (BE) were determined with respect to the position of the C 1 s peak at 284.8 eV. The residual pressure in the analysis chamber was maintained below 3 10^{-9} Torr during data acquisition. The new functionalized DPTH@MGO microstructures were observed by a JEOL JSM-840 scanning electron microscopy (SEM) (Tokyo, Japan) operated at 20 kV and a JEOL JEM-1400 transmission electron microscopy (TEM) (Tokyo, Japan).

2.2. Reagents and samples

For all experiments, high purity reagents were used. All plastic and glassware were cleaned with concentrated nitric acid and stored soaked in 10% (wt/wt) nitric acid; they were rinsed several times with water immediately before use. Doubly de-ionized water (DDW) (18 MΩ cm) obtained from a Milli-pore Milli-Q water system (Bedford, MA, USA) was used throughout.

For the synthesis of DPTH@MGO, 3-aminopropyltriethoxysilane, and diglutaric aldehyde were obtained from Fluka (Buchs, Switzerland). Brij 76C18EO10, tetraethoxysilane (TEOS), thiocarbonhydrazide, di-2-pyridil ketone, graphite,

$NaNO_3$ and $KMnO_4$ were purchased by Aldrich Chemie (Steinheim, Germany). Ethanol was supplied from Carlo Erba (Milano, Italy). Ferrous chloride tetrahydrate ($FeCl_2$ $4H_2O$), ferric chloride hexahydrate ($FeCl_3$ $6H_2O$), ammonium hydroxide 30% (wt/wt), methanol, sodium chloride and H_2SO_4 98% were obtained from Merck (Darmstadt, Germany) and H_2O_2 35% from Scharlab (Barcelona, Spain). Hydrochloric and nitric acid were supplied by Merck (Darmstadt, Germany). Standards 1000 mg L^{-1} for Au, Ag, Ir, Os, Pd, Pt, Sb and Hg solution Merck (Darmstadt, Germany) were used. Standards of working strength were made immediately prior to use by appropriate dilution as required.

A pH 3 buffer was prepared by mixing 50.0 mL of glycine 0.2 M Merck (Darmstadt, Germany) and 11.4 mL hydrochloric acid 0.2 M Merck (Darmstadt, Germany). A 2.6% (wt/vol) sodium tetra-hydroborate (III) (THB) Merck (Darmstadt, Germany) solution, prepared in 0.2% (wt/vol) NaOH Merck (Darmstadt, Germany), was used as reductant and a 2% (wt/vol) thiourea Merck (Darmstadt, Germany) solution in 4% (wt/wt) nitric acid was used as eluent.

The certified reference material (CRMs) analyzed to validate the proposed procedure was from National Research Council of Canada (NRCC) (Ontario, Canada): fortified Lake Water, TMDA 54.5. Seawater, mineral and tap water samples were collected from Málaga city in polypropylene bottles (previously cleaned by soaking for 24 h in 10% (wt/wt) nitric acid and finally rinsed thoroughly with DDW before use). Seawater samples were immediately filtered after collection by using a membrane of 0.45 μm pore size cellulose nitrate filters from Millipore (Bedford, MA, USA). After that, the samples were stored in low density polypropylene bottles at 4 ºC as recommended by Method 3010B from the Environmental Protection Agency (USA), for less than 3 days until analysis. For

the analysis of these samples, aliquots of 20 mL of sample were placed in volumetric flasks of 25 mL, then 2.5 mL of buffer of pH 3 and DDW were added up to the mark.

2.3. Synthesis of the functionalized MGO

The functionalized silica-coated MNPs (DPTH-MNPs) synthesis was described elsewhere [34]. GO was prepared according to the Hummers method modified [35,36] by chemical exfoliation of natural flake graphite followed by repeated purification cycles using centrifugation. The centrifugation steps were 5000 rpm (at 5 min) twice, 8000 rpm (at 5 min) once, 10000 rpm (at 5 min) once, 10000 rpm (at 10 min) once, and 11000 rpm (at 30 min) once. 10 g of natural graphite (99 wt% purity; average particle diameter -325 mesh (<44μm, ≥99 %), Aldrich Chemie (Steinheim, Germany)) was mixed with 7.5 g of $NaNO_3$ into a 2 L beaker. 600 mL of H_2SO_4 was added to the beaker and a magnetic stirrer chip. The mixture was stirred while cooling in an ice water bath. 40 g $KMnO_4$ was added gradually over a one-hour period. The cooling was continued for about 3 h, and the mixture was allowed to stand for five days at about 20 ºC with gentle stirring. 1 L of 5 % vol/vol H_2SO_4 aqueous solution was added over a 1 h stirring period, and stirring continued for 2 h. This was followed by addition of 30 mL H_2O_2 and further stirring for 2 h. Then, the centrifugation steps described above were addressed. After each centrifugation step, DDW was used to make up the volume in the centrifugation tubes.

The coupling of DPTH-MNPs with GO was conducted as follows: 500 mg of GO and 500 mg of DPTH-MNPs were mixed in DDW and stirred for 10 minutes. The mix was incubated at 65 ºC for 8 h. The obtained suspension was cooled to room

temperature and separated from the solution with the aid of external permanent magnet, washed with DDW and ethanol. Finally, the solid was dried at 80 ºC for 24 h. A schema of DPTH@MGO synthesized is showed in figure 1.

2.4. Study of the adsorption capacity

In order to evaluate the adsorption capacity of the new magnetic nanosorbent towards a high number of both toxic elements and elements of industrial and socio-economic interest, DPTH@MGO was evaluated as adsorbent in an in batch MSPE procedure with the determination of these elements by ICP OES. As is well known the adsorption capacity depends on the pH of the solution, so two different pHs, 5 and 8, were tested. The elements studied were As, Cr, Sb, Pb, Hg, Co, Cd, Cu, Ni, Zn, Ag, Au, Pd, Pt, Ir and Os. Standard solutions of 10 mg L^{-1} of As, Cr, Sb, Pb, Hg, Co, Cd, Cu, Ni and Zn were prepared in two 50 mL volumetric flask at pH 5 and 8 by meaning of 5 mL of buffers acetic acid/sodium acetate and boric acid/sodium borate. Other two 50 mL standard solutions of 10 mg L^{-1} of Ag, Au, Pd, Pt, Ir and Os at pH 5 and 8 were also prepared. Then, four portions of 50 mg of DPTH@MGO were weighted and placed in four 100 mL beakers where the prepared standard solutions were poured. The mixtures were dispersed by ultrasonication for 10 min at room temperature and after magnetically separated. The supernatants were measured for unextracted metal ions. The adsorption capacity towards each element was calculated by difference between the added and found concentration.

2.5. Optimization strategy

The FI-system configuration (Fig. 2) and the effect of different parameters on the adsorption and elution of Ag, Au, Ir, Os, Pd, Pt, Sb and Hg were studied to achieve

the best results. Two optimization strategies were used: multivariate by means surface designs with multiple response and univariate, changing one parameter and keeping the others constant.

The parameters optimized by multiple response surface designs using two central composite designs (CCD) [37], could be classified as: (1) chemical parameters relating to elution of Ag, Au, Ir, Os, Pd, Pt, Sb and Hg and reaction conditions for CVG and non-CVG; and (2) FI parameters for the simultaneous determination of the 8 elements. For each design, 16 experiments were required. These experiments were randomly performed. The response functions were the signal to noise ratio for the eight elements. The variables to be optimized in design (1) were concentrations of $NaBH_4$, thiourea and HNO_3. The concentration ranges studied for each factor were 0% and 4.0% for $NaBH_4$, 0% and 5.0% for thiourea and 0% and 10.0% for HNO_3. After this optimization, in design (2) sample, elution and reductant flow rates were varied by changing the speed of the peristaltic pumps (P1 and P2) and the inner diameter of the pump tubes. The lower and upper values given to the factors were 0.6 and 5.9 mL min^{-1} sample flow rate; 0.6 and 4.1 mL min^{-1} for eluent flow rate; and 0.6 and 2.6 mL min^{-1} for reductant flow rate.

The results of the experiments were processed by the statistical software Statgraphics Centurion XVI. The significance of the effects was checked by analysis of the variance (ANOVA).

2.6. Preconcentration and elution procedure

The FI manifold used for on-line preconcentration and elution of the eight elements is shown in Fig. 2. The FI system was operated as follows: during the 180 s sample loading period, valve in the “fill” position, a 5.6 mL min^{-1} flow of sample

(standard or blank) at pH 3 was pumped (via pump P1) through the reactor (located in the loop of the valve). The target analytes were retained on the sorbent reactor while the sample matrix components were directed to waste. At the beginning of the 99 s elution stage, the valve position was changed and the sample pump P1 was stopped. When the valve was in the "inject" position, the eluent passes through the reactor, thus, the accumulated analytes were eluted at an elution rate of 2.9 mL min^{-1} and merged with 2.6 mL min^{-1} flow of reductant in the MSIS. With this procedure, the FI system and the ICP OES instrument were coupled and operated completely synchronously. The automatic running program is shown in the supplementary material (SM), Table SM1.

3. Results and discussion

3.1. Characterization of DPTH@MGO

A detailed characterization of DPTH@MGO was carried out using XPS, FTIR, SEM and TEM measurements. The figures and tables obtained during the characterization are shown as SM.

The size, structure and surface morphology of the fabricated GO, DPTH-MNPs and DPTH@MGO were studied by TEM and SEM. TEM images for three materials are shown in SM 2 (A-C), (A) GO, (B) DPTH-MNPs and (C) DPTH@MGO. Nanosheets of GO can be observed in SM 2(A); and spherical nanoparticles dispersed on the GO sheets can be seen in SM 2(C). The size of these NPs was calculated of about 15–20 nm.

SEM micrographs have a large depth of field due to the very narrow electron beam, providing a characteristic three dimensional (3D) appearance useful for

understanding the surface structure of a sample. Back scattered electrons (BSE) are often used in analytical SEM to provide information about the distribution of different elements in the sample. The results of this study confirm the presence of nitrogen and sulphur in DPTH@MGO, therefore the synthesis could have been effective, SM 3. The results obtained from the spectrum shown in SM 3 are presented as a Table in SM 4. It is interesting that the nitrogen-to-sulphur ratio is quite similar than that predicted by theory (7:1). The structure of the DPTH can be seen in Figure 1.

In SM 5 (A–B), the XPS spectra of DPTH@MGO in the region of N and S are shown. In SM 5 (A), a double peak appears for S, this type of signal has been observed by other researches when employ adsorbents derived from thiourea [38]. This double peak is resulted from two tautomeric forms of the thiocarbonhidrazide (–C=S; –C–SH). In SM 5 (B) a peak appears for N.

The FT-IR spectrum (KBr pellets) is difficult due to the aromatic portion of the molecule produces numerous bands and the overlap makes difficult the detailed assignments. However, some assignments can be done in the mid-infrared region (Figure SM 6), the thiamides and MNPs band assignments were carried out from available data in bibliography[39,40]. All these studies confirm the success of the synthesis and functionalization.

3.2. Adsorption capacity

The results obtained from the study of the adsorption capacity of DPTH@MGO are shown in SM 7. Two elements were retained almost completely at both pHs, Ag and Au. PGMs were also retained in a high proportion (Ir only at acid pH), as well as, Sb and Hg. In general, the retention was higher at acid pH.

Taking advantage of capability of ICP OES to simultaneous multi-element detection, this technique was chosen to evaluate the useful of DPTH@MGO for the simultaneous extraction-preconcentration-determination of a large number of elements. Thus, the eight elements with good adsorption capacities (Sb, Hg, Ag, Au, Pd, Ir, Pt and Os) were selected to optimize a new on line MSPE-ICP OES method.

On the other hand, the adsorption capacity of un-functionalized GO towards the selected elements has been studied and compared with the adsorption capacity of DPTH@MGO, with a previous material synthesized by us (DPTH-MNPs) [34] and with other nanomaterial (nanometer-sized alumina functionalized with 3-(8-quinolinylazo)-4-hydroxybenzoic acid) [46]. In Table 2 it can be seen that the adsorption capacity of GO is quite lower. DPTH@MGO and DPTH-MNPs showed similar adsorption capacities for Pd and Ag, however three elements were retained by DPTH@MGO in higher proportion: Sb, Au and Pt. This study confirms that the preferential extraction mechanism is the formation of coordination complexes (chelates) through DPTH group. In the case of functionalized alumina, the results were similar, Au was retained in higher proportion on the alumina, the retention for Pd was similar and Ag was retained in higher proportion on DPTH@MGO.

3.3. Design of the flow injection system

First, the packing of DPTH@MGO into the KR previously designed by us for MNPs [34] was tested. The MGO magnetism properties compared to MNPs decreases when the GO content is higher than 5 wt% [41], as consequence, losses of DPTH@MGO were feared after several loading and elution cycles. However, the material was well retained by the magnets. A DPTH@MGO filled KR had to be re-filled only after 200

loading and elution cycles. This KR was located in the five-port rotatory valve of the FIAS- 400.

CVG atomic spectrometry is currently the most popular technique for the routine determination of trace amounts of elements which generate volatile species [24], in our case Hg and Sb. On the other hand, although noble metals hydrides are unstable and require rapid separation from the aqueous phase, their generation allows an alternative route for the introduction of these elements into atomic spectrometric atomizers [42]. For these reasons, a multimodal spray chamber, MSIS designed for ICP OES was chosen, this cyclonic spray chamber provides a way to generate chemical vapours inside of the chamber to be immediately introduced in the plasma, reducing contact times of the vapours with the solution. A scheme of the FI manifold used was shown in Figure 2.

3.4. Optimization procedure

Multiple response central composite designs were employed in order to obtain compromise conditions for simultaneous determination, although some of parameters were optimized in a univariate way, e.g. pH.

3.4.1. Effect of pH

Since the pH affects the extent of complexation of the different ions on the DPTH@MGO KR, this parameter was the first to be optimized. For this study, standard solutions of 100 μg L^{-1} of the target analytes were prepared at different pHs. The pH was studied in the range between 1.0 to 11.0. The pH ≤ 2 was adjusted with diluted HCl; from 2.0 to 5.0 were adjusted using glycine–HCl and sodium acetate–acetic acid buffer; from 5.0 to 10.0 using borax-boric acid buffer and pH ≥ 10 was adjusted using NaOH. The results of this study are shown as SM, In Figure SM 8(A) were displayed

the elements with higher emission intensity and in Figure SM 8(B) the elements with lower emission intensity. As can be seen in these figures all the elements, except Ag, showed some maximum at pH 3. Pd presents only a maximum at this pH, being one of the elements with lower emission intensity, thus in order to select a pH value that provides the simultaneous multielemental determination, a pH 3.0 was chosen as the optimum.

3.4.2. Effect of eluent and reductant

For these experiments, standard solutions were prepared containing 100 μg L^{-1} of the target analytes. The concentrations of reductant ($NaBH_4$), HNO_3 and thiourea were considered to be dependent variables and the effects of these were studied by applying a CCD involving 16 runs in order to obtain the optima conditions. The three dimensional representation is presented in Fig.3. The data indicate that interactions usually occur between principal factors. This means that the response surfaces in the factorial space are curved in the domain of the experimental design. From the results showed in Fig. 3, the software provided the conditions to obtain the highest desirability: 2.1% Thiourea (wt/vol), 6.5 % HNO_3 (wt/vol) and 2.5% $NaBH_4$ (wt/vol).

NaOH solution was used to stabilize $NaBH_4$ by preventing its adverse reaction with water during storage. Then, the influence of NaOH concentration was studied between 0.1% and 0.5% (wt/vol) for a concentration of $NaBH_4$ 2.5% (wt/vol). The best S/N signals were obtained with 0.2% NaOH because an excessive increase in NaOH concentration decreases the acidity of the reaction mixture and hence, the reaction rate of hydride generation. For further experiments, the concentration of NaOH was fixed in 0.2% (wt/vol).

3.4.3. Effect of sample, eluent and reductant flow rate

For these experiments, standard solutions were prepared containing 100 μg L^{-1}. These are three important parameters. The sample flow rate should be optimized to ensure quantitative retention along with minimization of the time required for sample processing. The volume of eluent has a significant influence on the preconcentration factor; hence, the volume of the eluent must be as low as possible to achieve the highest enrichment factor. Additionally, the flow rates of the sample and eluent solutions are two important factors for the quantitative recoveries and desorption of target chelates during solid phase extraction studies.

As has been said, their effects were studied by applying a multiple response CCD involving 16 runs in order to determine the optimal conditions for sample, eluent and reductant flow rates. The desirability graph for the multiple responses of all the elements is shown in Fig. 4. Based on these results, the statistical software provided the optimal conditions: sample flow rate of 5.6 mL min^{-1}, an eluent flow rate of 2.9 mL min^{-1}, and a reductant flow rate of 2.6 mL min^{-1}.

3.4.4. Selection of Ar purge flow and reagents flows (for nebulization and vapour generation)

Taking into account the optimum conditions previously described, the Ar flow was studied with a solution containing 100 μg L^{-1} of Ag, Au, Ir, Os, Pd, Pt, Hg and Sb. The standard solution was measured together with the blanks; in different conditions varying Ar flow from 0.4 to 1 L min^{-1} (higher Ar flow rates extinguish the plasma). An Ar flow rate of 0.6 L min^{-1} was chosen in order to achieved the simultaneous determination of the analytes.

3.4.5. Pre-concentration time

The loading or pre-concentration time directly affects the enrichment factor and the sensitivity. The sensitivity increases on increasing the sample loading time, however the sample frequency decreases. The preconcentration time was studied between 60 s and 420 s for each element, using the optimum chemical and FI optimized conditions. The signals intensities increased practically linear up to 5 min for all of the analytes. The loading time was set to 180 s to achieve a high sample frequency with a reasonable sensitivity. Longer loading times can be used for samples with low analyte concentrations.

3.5. Performance of the method

Under the optimum conditions described above, performance data of the on-line MSPE-MSIS-ICP-OES system for simultaneous determination of Au, Ag, Pt, Pd, Ir, Os, Sb, and Hg were obtained. For 3 min pre-concentration time and a sample flow rate of 5.6 mL min^{-1}, the linear calibration graph for each analyte are shown in Table 2. A complete cycle of the FI-operation is ca. 279 s per analyte, the 8 target analytes in a sample can be determined with a throughput of about 13 h^{-1}.

The detection (LOD) and quantification limits (LOQ) are defined as 3 s (n=11) and 10 s (n=11) respectively; the precision for aqueous standards, evaluated as the relative standard deviation obtained after analysing a standard of 25 μg l^{-1} of the 8 target analytes (11 replicates) and the enrichment factor EF, defined as the ratio of the slopes of the linear section of the calibration graphs with and without pre-concentration (changing the KR by another unfilled) are shown in Table 2. The EFs and determination limits can be improved by increasing the pre-concentration time which can be increased at least up to 5 min.

For comparison purposes, the analytical performance data of similar methods reported in the literature are listed in Table 3. Although it is difficult to compare the figures of merit for the developed method directly with results from other workers, because of different experimental conditions such as type of packing (in mini-column or KR), amount of adsorbent, sample flow rate, etc., some estimation can be made. As can be seen, generally the detection limits for the target elements and the precisions of the developed method were better or similar that those reported in the literature. The method shown in this work allows the analysis of both easy and difficult forming chemical vapours, such as Hg, Sb and noble metals, respectively. Furthermore, it is one of the methods which determine higher number of elements simultaneously, 8 elements with a high sample throughput, 13 h^{-1}. If 180 s are used as loading time, the sample consumption is 16.8 mL (5.6 mL min^{-1} x 3 min) and only 50 mg of DPTH@MGO were necessary for 200 measurements. The low consumption of sample and reagent fits this method within the Green Analytical Chemistry.

3.6. Analytical application

The proposed procedure was validated through the determination of 8 target analytes in a certified reference material TMDA 54.5 Fortified Lake Water. As shown in Table 4, no significant differences were observed, for p=0.05 when comparing the values obtained by the proposed method and certified values (t-test for a 95% confidence level). Because this standard reference sample has included trace elements such as transition metals, it can be said that there is not any interference from these metals at μg L^{-1} concentrations. Additionally, an alternative validation process was conducted through recovery assays Table 4. These assays were also made for TMDA 54.5 and for mineral water, tap water and seawater samples collected locally. As can be

seen in Table 4, the recoveries for the spiked samples were near to 100%. These results indicate that the presented method is valuable to apply to the multielement determination of trace noble metals, Sb and Hg in samples with very complex matrix such as seawater samples (high salinity approximately 35.5 g L^{-1}).

4. Conclusions

The pre-concentration and separation system using DPTH@MGO as a sorbent material has been evaluated and demonstrated to be promising for routine determination of the trace amounts of Au, Ag, Pt, Pd, Ir, Os, Sb, and Hg in environmental and seawater samples. The main advantages of the proposed method are that the method is rapid, easy to use, automatic and selective with good analytical characteristics, low LODs and LOQs and high EF, compared with other similar methods. In general, the implementation of on line MSPE systems offer several important benefits such as simplicity of operation, high sample throughput, improved analytical characteristics and reduced sample and reagent consumption. To our knowledge and up to date, this is the first MSPE method online that uses functionalized MGO as an adsorbent.

Acknowledgements

The authors would like to thank Amparo García de Torres and José Manuel Cano Pavón for their advices during the development of this work. This work has been partially supported by the University of Málaga (Proyecto Puente UMA), FEDER funds and Junta de Andalucía.

Authors declare that there are no conflicts of interest

References

[1] S. Chowdhury, R. Balasubramanian, Recent advances in the use of graphene-family nanoadsorbents for removal of toxic pollutants from wastewater, Adv. Colloid. Interface Sci. 204 (2014) 35–56, https://doi.org/10.1016/j.cis.2013.12.005.

[2] X. Wang, B. Liu, Q. Lu, Q. Qu, Graphene-based materials: fabrication and application for adsorption in analytical chemistry, J. Chromatogr. A. 1362 (2014) 1-15, https://doi.org/10.1016/j.chroma.2014.08.023.

[3] J.G. Yu, L.Y. Yu, H. Yang, Q. Liu, X.H. Chen, X.Y. Jiang, X.Q. Chen, F.P. Jiao, Graphene nanosheets as novel adsorbents in adsorption, preconcentration and removal of gases, organic compounds and metal ions, Sci. Total Environ. 502 (2015) 70–79, https://doi.org/10.1016/j.scitotenv.2014.08.077.

[4] S. Wu, K. Zhang, X. Wang, Y. Jia, B. Sun, T. Luo, F. Meng, Z. Jin, D. Lin, W. Shen, L. Kong, J. Liu, Enhanced adsorption of cadmium ions by 3D sulfonated reduced graphene oxide, Chem, Eng. J. 262 (2015) 1292–1302, https://doi.org/ 10.1016/j.cej.2014.10.092.

[5] S. Luo, X. Xu, G. Zhou, C. Liu, Y. Tang, Y. Liu, Amino siloxane oligomer-linked graphene oxide as an efficient adsorbent for removal of Pb(II) from wastewater, J, Hazard, Mater. 274 (2014) 145–155, https://doi.org/10.1016/j.jhazmat.2014.03.062.

[6] F. Fang, L. Kong, J. Huang, S. Wu, K. Zhang, X.g. Wang, B. Sun, Z. Jin, J. Wang, X.J. Huang, J. Liu, Removal of cobalt ions from aqueous solution by an amination graphene oxide nanocomposite, J. Hazard. Mater. 270 (2014) 1–10, https://doi.org/10.1016/j.jhazmat.2014.01.031.

[7] Z. Xu, Y. Zhang, X. Qian, J. Shi, L. Chen, B. Li, J. Niu, L. Liu, One step synthesis of polyacrylamide functionalized graphene and its application in Pb(II) removal, Appl. Surf. Sci. 316 (2014) 308–314, https://doi.org/10.1016/j.apsusc.2014.07.155.

[8] M.H. Mashhadizadeh, Z. Karami, Solid phase extraction of trace amounts of Ag, Cd, Cu, and Zn in environmental samples using magnetic nanoparticles coated by 3-(trimethoxysilyl)-1-propantiol and modified with 2-amino-5-mercapto-1,3,4-thiadiazole and their determination by ICP-OES, J. Hazard. Mater. 190 (2011) 1023-1029, https://doi.org/10.1016/j.jhazmat.2011.04.051.

[9] A.E. Karatapanis, Y. Fiamegos, C.D. Stalikas, Silica-modified magnetic nanoparticles functionalized with cetylpyridinium bromide for the preconcentration of metals after complexation with 8-hydroxyquinoline, Talanta 84 (2011) 834-839, https://doi.org/10.1016/j.talanta.2011.02.013.

[10] Q. Han, Z. Wang, J. Xia, S. Chen, X. Zhang, M. Ding, Facile and tunable fabrication of Fe3O4/graphene oxide nanocomposites and their application in the magnetic solid-phase extraction of polycyclic aromatic hydrocarbons from environmental water samples, Talanta 101 (2012) 388-395, https://doi.org/10.1016/j.talanta.2012.09.046.

[11] S.D. Pan, L.X. Zhou, Y.G. Zhao, X.H. Chen, H.Y. Shen, M.Q. Cai, M.C. Jin, Amine-functional magnetic polymer modified graphene oxide as magnetic solid-phase extraction materials combined with liquid chromatography-tandem mass spectrometry for chlorophenols analysis in environmental water, J. Chromatogr. A, 1362 (2014) 34-42. https://doi.org/ 10.1016/j.chroma.2014.08.027.

[12] W. Ji, M. Zhang, W. Duan, X. Wang, H. Zhao, L. Guo, Phytic acid-stabilized super-amphiphilic Fe_3O_4-graphene oxide for extraction of polycyclic aromatic hydrocarbons from vegetable oils, Food Chem. 235 (2017) 104–110, https://doi.org/10.1016/j.foodchem.2017.05.054.

[13] J.-B. Ma, L.-M. Zhao, Q.-H. Rui, Y-F. Lian, Y.-M. Chen, J. Xu, Y. Zhu, Y.-G. Zhao, Application of carbon nanosorbent for PRiME pass-through cleanup of 10

selected local anesthetic drugs in human plasma samples, Anal. Chim. Acta 960 (2017) 72-80.

[14] J.-B. Ma, H.-W. Qiu, Q.-H. Rui, Y.-F. Liao, Y.-M. Chen, J. Xu, Y. Zhang, Y. Zhu, Y.-G. Zhao, Enhanced cleanup efficiency hydroxyl functionalized-magnetic graphene oxide and its comparison with magnetic carboxyl-graphene for PRiME pass-through cleanup of strychnine and brucine in human plasma samples, Anal. Chim. Acta 1020 (2018) 41-50.

[15] E. Ziaei, A. Mehdinia, A. Jabbari, A novel hierarchical nanobiocomposite of graphene oxide-magnetic chitosan grafted with mercapto as a solid phase extraction sorbent for the determination of mercury ions in environmental water samples, Anal. Chim. Acta 850 (2014) 49-56, https://doi.org/10.1016/j.aca.2014.08.048.

[16] S.W. Su, B. Chen, M. He, B. Hu, Z. Xiao. Determination of trace/ultratrace rare earth elements in environmental samples by ICP-MS after magnetic solid phase extraction with Fe3O4@SiO2@polyaniline-graphene oxide composite, Talanta, 119 (2014) 458-466, https://doi.org/10.1016/j.talanta.2013.11.027.

[17] E. Aliyari, M. Alvand, F. Shemirani, Simultaneous separation and preconcentration of lead and cadmium from water and vegetable samples using a diethylenetriamine-modified magnetic graphene oxide nanocomposite, Anal. Methods 7 (2015) 7582-7589, https://doi.org/10.1039/C5AY01088H.

[18] A. Islam, H. Ahmad, N. Zaidi, S. Kumar, A graphene oxide decorated with triethylenetetramine-modified magnetite for separation of chromium species prior to their sequential speciation and determination via FAAS, Microchim. Acta 183 (2016) 289-296, https://doi.org/10.1007/s00604-015-1641-2.

[19] E. Yavuz, Ş. Tokalıoğlu, Ş. Patat, Magnetic dispersive solid phase extraction with graphene/ZnFe2O4 nanocomposite adsorbent for the sensitive determination of mercury in water and fish samples by cold vapor atomic absorption spectrometry, Microchem. J. 142 (2018) 85-93. https://doi.org/ 10.1016/j.microc.2018.06.019.

[20] S. Ozdemir, S.A. Mohamedsaid, E. Kilinc, A. Yıldırımd, M. Soylak, Application of magnetized fungal solid phase extractor with Fe_2O_3 nanoparticle for determination and preconcentration of Co(II) and Hg(II) from natural water samples, Microchem. J. 143 (2018) 198-204. https://doi.org/10.1016/j.microc.2018.07.032.

[21] E. Öztürk Er, E. Maltepe, S. Bakirdere, A novel analytical method for the determination of cadmium in sorrel and rocket plants at ultratrace levels: Magnetic chitosan hydrogels based solid phase microextraction-slotted quartz tube-flame atomic absorption spectrophotometry, Microchem. J. 143 (2018) 393-399. https://doi.org/10.1016/j.microc.2018.08.019.

[22] Y. Yamini, M. Safari, Modified magnetic nanoparticles with catechol as a selective sorbent for magnetic solid phase extraction of ultra-trace amounts of heavy metals in water and fruit samples followed by flow injection ICP-OES, Microchemical Journal, 2018, 143, 503-511. https://doi.org/10.1016/j.microc.2018.08.018.

[23] A.L. de Toffoli, E. Vasconcelos Soares Maciel, B. Henrique Fumes, F.M. Lanças, The role of graphene-based sorbents in modern sample preparation techniques, J. Sep. Sci. 41 (2018) 288–302, https://doi.org/10.1002/jssc.201700870.

[24] P. Wu, L. He, C. Zheng, X. Hou, R.E. Sturgeon, Applications of chemical vapor generation in non-tetrahydroborate media to analytical atomic spectrometry, J. Anal. Spectrom. 25 (2010) 1217-1246, https://doi.org/10.1039/C003483E.

[25] R.L.J. McLaughlin, I.D. Brindle, A new sample introduction system for atomic spectrometry combining vapour generation and nebulization capacities, J. Anal. At. Spectrom. 17 (2002) 1540-1548, https://doi.org/10.1039/B208011G.

[26] M. Angelone, M. Udovic, Potentially harmful elements in urban soils. In: Bini, C., Bech, J. (Eds.), PHEs, Environment and Human Health: Potentially Harmful Elements in the Environment and the Impact on Human Health. Springer Netherlands, Dordrecht, 2014. pp. 221–251, https://www.springer.com/us/book/9789401789646.

[27] F. Zereini, C.L.S. Wiseman, Platinum Metals in the Environment, Springer Verlag, Berlin, Heidelberg; 2015, https://www.springer.com/us/book/9783662445587.

[28] V.M. Goldschmidt, The principles of distribution of chemical elements in minerals and rocks, J. Chem. Soc. (1937) 655–673, https://doi.org/ 10.1039/JR9370000655.

[29] T.E. Graedel, The prospects for urban mining, The Bridge, 41 (1) (2011) 43–50, https://www.nae.edu/File.aspx?id=43182&v=e31338e1

[30] http://ec.europa.eu/growth/sectors/raw-materials/specific-interest/critical_en

[31] R. Cornelis, H. Crews, J. Caruso, K.G. Heumann, editors, Handbook of Elemental Speciation II: Species in the Environment, Food, Medicine & Occupational Health. John Wiley & Sons Ltd., Chichester; 2005. pp. 47–68, https://www.wiley.com/.../Handbook+of+Elemental+Speciation+II.

[32] S. Sundar, J. Chakravarty. Antimony toxicity, Int. J. Environ. Res. Public Health, 7 (2010) 4267-4277, https://doi.org/10.3390/ijerph7124267.

[33] K.M. Rice, E.M. Walker Jr, M. Wu, C. Gillette, E.R. Blough, Environmental mercury and its toxic effects, J. Prev. Med. Public Health, 47 (2014) 74–83, https://doi.org/10.3961/jpmph.2014.47.2.74.

[34] E. Vereda Alonso, M.M. López Guerrero, P. Colorado Cueto, J. Barreno Benítez, J.M. Cano Pavón, A. García de Torres, Development of an on-line solid phase extraction method based on new functionalized magnetic nanoparticles. Use in the determination of mercury in biological and sea-water samples, Talanta, 153 (2016) 228-239, https://doi.org/10.1016/j.talanta.2016.03.027.

[35] W.S. Hummers, R.E. Offeman, Preparation of graphitic oxide, J. Am. Chem. Soc. 80 (1985) 1339–1339, https://doi.org/10.1021/ja01539a017.

[36] P.N. Diagboya, B.Y. Olu-Owolabi, D. Zhou, B.H. Han, Graphene oxide-tripolyohosphate hybrid used as a potent sorbent for cationic dyes, Carbon. 79 (2014) 174–182, https://doi.org/10.1016/j.carbon.2014.07.057.

[37] J. Goupy, Plans D'expériences Pour Surfaces de Réponse, Dunod, Paris, France; 1999,

[38] G. Cheng, M. He, H. Peng, B. Hu, Dithizone modified magnetic nanoparticles for fast and selective solid phase extraction of trace elements in environmental and biological samples prior to their determination by ICP-OES, Talanta 88 (2012) 507–515, https://doi.org/10.1016/j.talanta.2011.11.025.

[39] E. Pretsch, T. Clerc, J. Seibl, W. Simon, Tablas para la elucidación estructural de compuestos orgánicos por métodos espectroscópicos, Alhambra, Madrid, Spain; 1985.

[40] E.P. García Casillas, C.A. Rodríguez González, C.A. Martínez Pérez, Infrared spectroscopy of functionalized magnetic nanoparticles, in: Theophanides Theophile (Ed.), Infrared Spectroscopy – Materials Science, Engineering and Technology; 2012. pp. 405–420, https://doi.org/10.5772/35481.

[41] M.A. Majidi, Y. Wicaksono, A.D. Fauzi, A. Taufik, R. Saleh, A. Rusydi, Theoretical investigation on the magnetization enhancement of Fe_3O_4-reduced

graphene oxide nanoparticle system. IOP Conf. Series: Materials Science and Engineering, 188 (2017) 012033, https://doi.org/10.1088/1757-899X/188/1/012033.

[42] A. Calvo Fornieles, A. García de Torres, E. Vereda Alonso, J.M. Cano Pavón, Simultaneous determination of traces of Pt, Pd, and Ir by SPE-ICP-OES. Test for chemical vapor generation, Microchem. J. 124 (2016) 82-89, https://doi.org/10.1016/j.microc.2015.07.024.

[43] C.B. Chen, Z. Zhuang, X. Wang, F.S.C. Lee, Cold vapour generation technique for the determination of some noble metals using movable reduction bed coupled with inductively coupled plasma mass spectrometry (ICP/MS), Anal. Sci. 17 (2001) 275-277.

[44] H. Matusiewicz, M. Slachcinski, Method development for simultaneous multi-element determination of transition (Au, Ag) and noble (Pd, Pt, Rh) metal volatile species by microwave induced plasma spectrometry using a triple-mode microflow ultrasonic nebulizer and in situ chemical vapor generation, J. Anal. At. Spectrom. 25 (2010) 1324-1333, https://doi.org/10.1039/C002886J.

[45] H. Matusiewicz, M. Slachcinski, Method development for simultaneous determination of transition (Au, Ag, Cd, Cu, Mn, Ni, Pb, Zn) and noble (Pd, Pt, Rh) metal volatile species by microwave-induced plasma spectrometry using Ultrasonic Micronebulizer Dual Capillary Sample Introduction System, Spectrosc. Lett. 43 (2010) 172-182, https://doi.org/10.1080/00387010903284323.

[46] C. Hang, B. Hu, Z. Jiang, N. Zhang, Simultaneous on-line preconcentration and determination of trace metals in environmental samples using a modified nanometer-sized alumina packed micro-column by flow injection combined with

ICP-OES, Talanta 71 (2007) 1239-1245, https://doi.org/10.1016/j.talanta.2006.06.033.

[47] Z. Fan, Z. Jiang, F. Yang, B. Hu, Determination of platinum, palladium and rhodium in biological and environmental samples by low temperature electrothermal vaporization inductively coupled plasma atomic emission spectrometry with diethyldithiocarbamate as chemical modified, Ana.l Chim. Acta 510 (2004) 45-51, https://doi.org/10.1016/j.aca.2003.12.055.

[48] S. Barua, I.M.M. Rahman, M. Miyaguchi, A.S. Mashio, T. Maki, H. Hasegawa, On-site analysis of gold, palladium, or platinum in acidic aqueous matrix using electrode plasma-optical emission spectrometry combined with ion-selective preconcentration, Sens. Actuators B Chem. 272 (2018) 91-99, https://doi.org/10.1016/j.snb.2018.05.132.

[9]

Figure captions

Figure 1. DPTH@MGO

Figure 2. FI system schematic diagram for preconcentration step (A) and elution step (B). P1 and P2, peristaltic pumps; W, waste; S, sample; R, reductant; and E, eluent.

Figure 3. Response surface obtained for the simultaneous optimization of the eluent and reductant concentrations for the simultaneous determination of Au, Ag, Pt, Pd, Ir, Os, Sb, and Hg.

Figure 4. Response surface obtained for the simultaneous optimization of the sample, elution and reductant flow rates for simultaneous determination of Au, Ag, Pt, Pd, Ir, Os, Sb, and Hg.

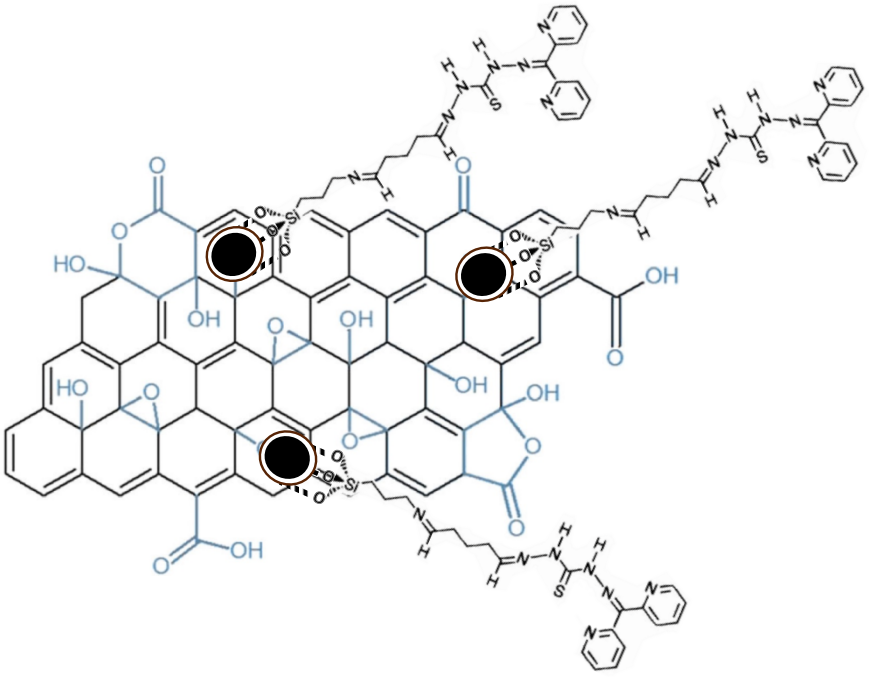

Figure 1

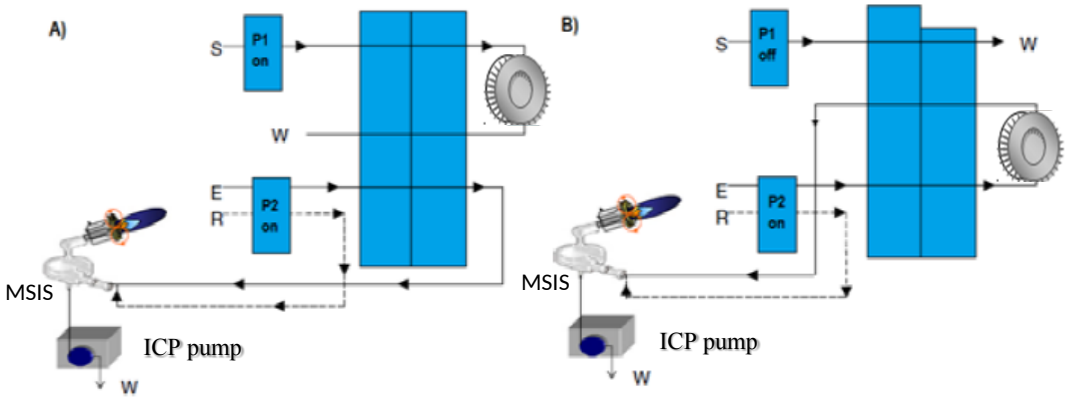
A)
S
P1
on
W
E
R
P2
on
MSIS
ICP pump
W
B)
S
P1
off
W
E
R
P2
on
MSIS
ICP pump
W

Figure 2

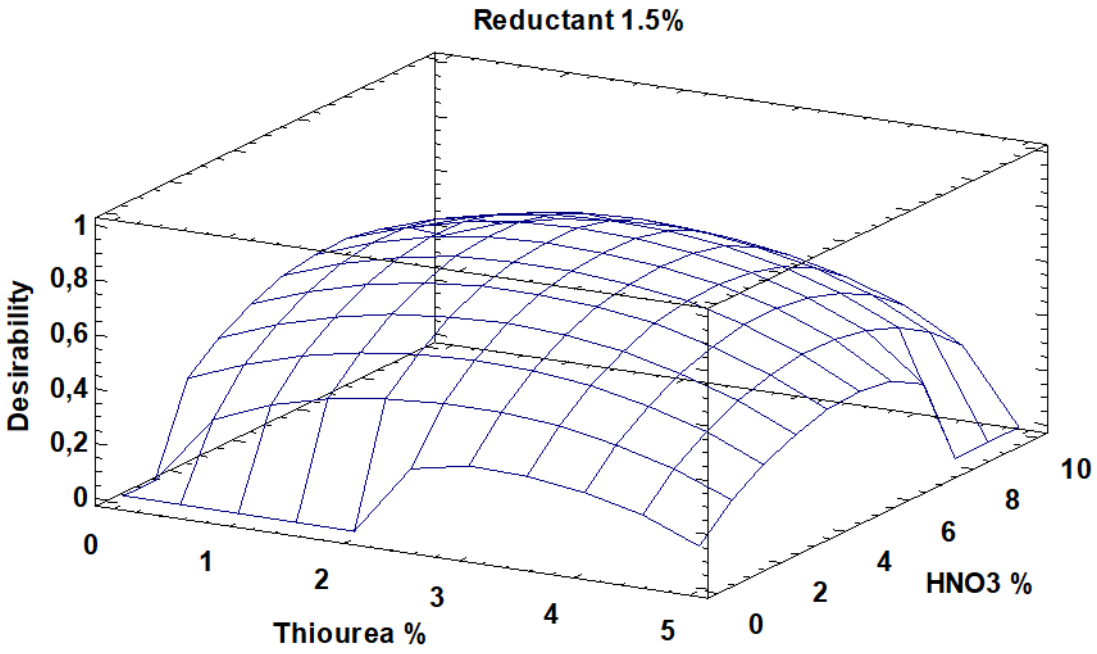
Reductant 1.5%
Desirability
1
0,8
0,6
0,4
0,2
0
0
1
2
3
4
5
Thiourea %
0
2
4
6
8
10
HNO3 %

Figure 3

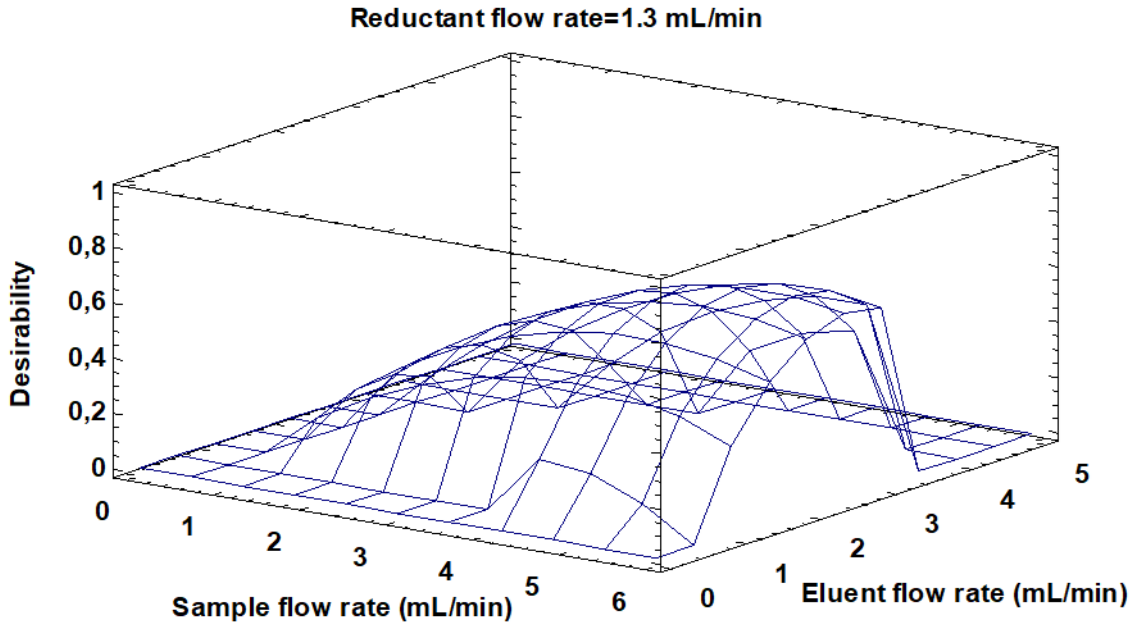
Reductant flow rate=1.3 mL/min
Desirability
1
0,8
0,6
0,4
0,2
0
0
1
2
3
4
5
6
Sample flow rate (mL/min)
0
1
2
3
4
5
Eluent flow rate (mL/min)

Figure 4

Table 1

Operating conditions for Optima 7300 DV ICP OES

Nebulizer Ar flow rate, L min^{-1}	0.6
Auxiliary Ar flow rate, L min^{-1}	0.2
Plasma Ar flow rate, L min^{-1}	15
Incident power, kW	1.3
Number of replicates	3
Distance from FIAS-400 to ICP OES	14 cm

Table 2

Comparison of adsorption capacities with other sorbent

Element	DPTH@MGO (mg/g)	GO (mg/g)	DPTH-MNPs [34] (mg/g)	Nanometer-sized alumina [46] (mg/g)
Pt	4.50	--	0.39	No reported
Pd	6.50	0.25	7.71	7.6
Ir	7.42	--	10.00	No reported
Os	6.42	--	9.00	No reported
Ag	9.72	0.15	9.10	5.1
Au	9.25	0.02	6.22	17.7
Sb	8.07	--	6.00	No reported
Hg	5.82	0.24	5.19	No reported

Table 3

Analytical performance

	Wavelengths (nm)	Blank signal	LOD (µg/L)	LOQ (µg/L)	Calibration curves	linear calibration (µg/L)	RSD (%)	E.F.
Pt	214.423	227 ± 22	0.4	2.8	y = 62.441x + 268.22	2.8-5000	3.8	28
Pd	340.458	-77 ± 48	2.6	8.3	y = 59.505x – 90.440	8.3-5000	4.0	6
Ir	224.268	132 ± 30	0.2	6.5	y = 33.363x + 213.82	6.5-400	3.1	9
Os	228.226	180 ± 43	1.2	7.7	y = 45.782x + 256.03	7.7-400	3.8	33
Ag	338.289	631 ± 116	0.5	3.0	y = 319.53x + 826.30	3.0-5000	3.2	22
Au	267.595	136 ± 45	0.6	4.8	y = 74.089x + 229.44	4.8-3500	2.6	29
Sb	206.836	155 ± 20	1.5	9.0	y = 18.440x + 185.81	9.0-5000	4.5	9
Hg	253.652	-555 ± 30	0.05	0.2	y = 1304.0x - 533.59	0.2-1000	1.6	3

Table 4

A comparison of analytical performance data with literatures

Techniques	Preconcentration method	Nº of analytes	Limits of detection (µg L^{-1})								% RSD	Ref.
			Ag	Au	Ir	Os	Pd	Pt	Sb	Hg		
ICP OES	DPTH-gel	3	-	-	0.6	-	0.5	1.4	-	-	2.7-2.9	[42]
ICP MS[a]	CVG	4	17.7	1.6	-	-	3.3	1.7	-	-	5	[43]
MIP OES[b]	Microflow Ultrasonic Nebulizer	5	1.5	1.2	-	-	1.1	2.9	-	-	7-8	[44]
MIP OES[b]	Microflow Ultrasonic Nebulizer	11	1.75	2.49	-	-	2.01	7.65	-	-	8-12	[45]
ICP OES	Nanometer-sized alumina	6	0.12	0.27	-	-	0.44	-	-	-	1.6-4.5	[46]
ICP OES	ETV[c]	3	-	-	-	-	1.4	5.4	-	-	1.4-2.6	[47]
LEP OES[d]	Macrocycle equipped SPE	3	-	0.8	-	-	3.1	57.3	-	-	≤ 5	[48]
ICP OES	DPTH@MGO (on line)	8	0.5	0.6	0.2	1.2	2.6	0.4	1.5	0.05	1.6-4.5	This work

[a] Inductively coupled plasma mass spectrometry; [b]Microwave induced plasma optical emission spectrometry; [c] Electrothermal vaporization; [d]Liquid electrode plasma optical emission spectrometry

Table 5. Analytical applications, certified material.

Sample	Found (µg L^{-1})								Recovery (%)							
	Ag	**Au**	**Ir**	**Os**	**Pd**	**Pt**	**Sb**	**Hg**	**Ag**	**Au**	**Ir**	**Os**	**Pd**	**Pt**	**Sb**	**Hg**
TMDA 54.5	13 ± 1 (13.3±1.42) †	-	161 ± 4	-	-	361.7 ± 0.2	27.8 ± 0.4 (27.8±2.26) †	-	98†	-	-	-	-	-	100†	-
Spiked 30 µg L^{-1}	41 ± 5	31.1 ± 0.6	195 ± 4	30.53 ± 0.08	31.9 ± 0.1	393.1 ± 0.4	56 ± 4	28.5 ± 0.5	93	104	113	102	106	105	94	95
Spiked 40 µg L^{-1}	55 ± 2	39.2 ± 0.1	198 ± 4	39.6 ± 0.6	38.6 ± 0.1	396 ± 4	70 ± 2	41.1 ± 0.1	105	98	93	99	97	86	106	103
Mineral Water	-	-	-	-	-	-	-	-	-	-	-	-	-	-	-	-
Spiked 30 µg L^{-1}	30.53 ± 0.02	30.6 ± 0.2	28.60 ± 0.04	28.4 ± 0.8	30.13 ± 0.03	28 ± 0.2	33 ± 2	28 ± 3	102	102	95	95	100	93	110	93
Spiked 40 µg L^{-1}	42.0 ± 0.5	40.1 ± 0.8	39 ± 6	41 ± 3	41 ± 1	40.8 ± 0.5	38 ± 2	41.8 ± 0.2	105	100	98	103	103	102	95	105
Tap Water	-	-	-	-	-	-	-	-	-	-	-	-	-	-	-	-
Spiked 20 µg L^{-1}	18 ± 1	18.1 ± 0.5	20 ± 1	18 ± 2	20 ± 3	21.2 ± 1.1	23.3 ± 0.6	19.1 ± 0.4	90	91	100	90	100	106	117	96
Spiked 30 µg L^{-1}	31.94 ± 0.04	29 ± 3	29.6 ± 0.1	30.70 ± 0.04	30 ± 3	30.25 ± 0.04	27.8 ± 0.2	30.6 ± 0.2	106	97	99	102	100	101	93	102
Sea Water 1	-	-	-	-	-	-	-	-	-	-	-	-	-	-	-	-
Spike1	51 ± 6	49.0 ± 0.2	78 ± 9	76 ± 9	49 ± 2	74 ± 12	55 ± 1	50 ± 1	102	98	98	95	98	93	110	100
Spike2	60 ± 2	60.8 ± 0.4	91.61 ± 0.05	93.2 ± 0.1	62 ± 1	95.7 ± 0.2	56 ± 15	60 ± 5	100	101	102	104	103	106	93	100
Sea Water 2	-	11±3	-	-	4*	32 ± 4	-	-	-	-	-	-	-	-	-	-
Spike3	37 ± 3	47 ± 1	65 ± 6	56 ± 13	42 ± 3	111 ± 5	47 ± 1	38 ± 1	93	90	108	93	95	99	94	95
Spike4	52 ± 3	60 ± 2	75 ± 1	82 ± 3	54 ± 3	132 ± 9	61 ± 10	48 ± 1	104	98	94	103	100	100	102	96

†Certified concentration (µg L^{-1}) for TMDA 54.5 and Concordance (%)
*indicative value (<LOQ)
Sea Water 1 (Harbour of Malaga)
Sea Water2 (Torrox Costa)
Spike1 (50 µg L^{-1} Ag, Au, Pd, Sb, Hg, and 80 µg L^{-1} Ir, Os, Pt,)
Spike2 60 µg L^{-1} Ag, Au, Pd, Sb, Hg, and 90 µg L^{-1} Ir, Os, Pt,)
Spike3 (40 µg L^{-1} Ag, Au, Pd, Hg, 50 µg L^{-1} Sb, 60 µg L^{-1} Ir, Os, and 80 µg L^{-1} Pt)
Spike4 (50 µg L^{-1} Ag, Au, Pd, Hg, 60 µg L^{-1} Sb, 80 µg L^{-1} Ir, Os, and 100 µg L^{-1} Pt)

Table SM 1

Automatic running program of the FI system

Step	Pump	Solution	Valve position	Flow rate/ mL min^{-1}	Time/s	Direction
Sample loading period	P1	Sample	1	5.6	180	Waste
	P2	HNO_{3+}Tiourea/ $NaBH_4$	1	2.9/2.6	180	Waste
Elution	P1	-	2	0	99	ICP-OES
	P2	HNO_{3+}Tiourea/ $NaBH_4$	2	2.9/2.6	99	ICP-OES

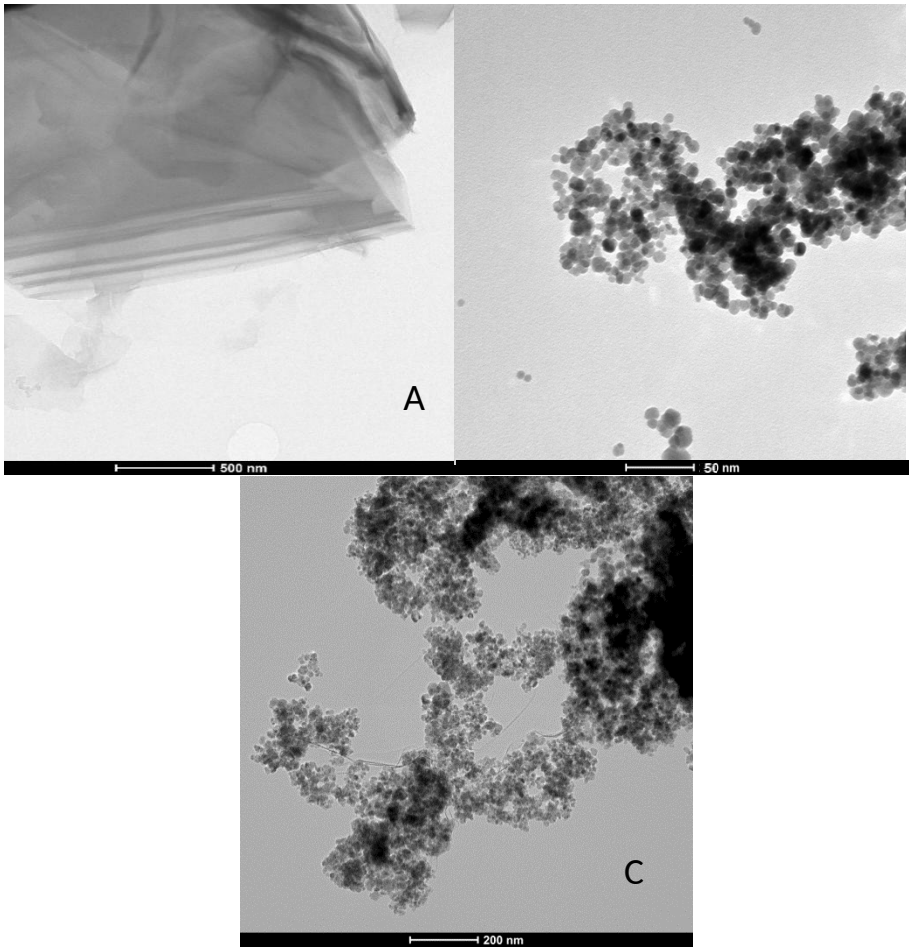

SM2. TEM images (A) GO scale 500 nm. (B) DPTH-MNPs scale 50 nm. (C) DPTH@MGO scale 200 nm.

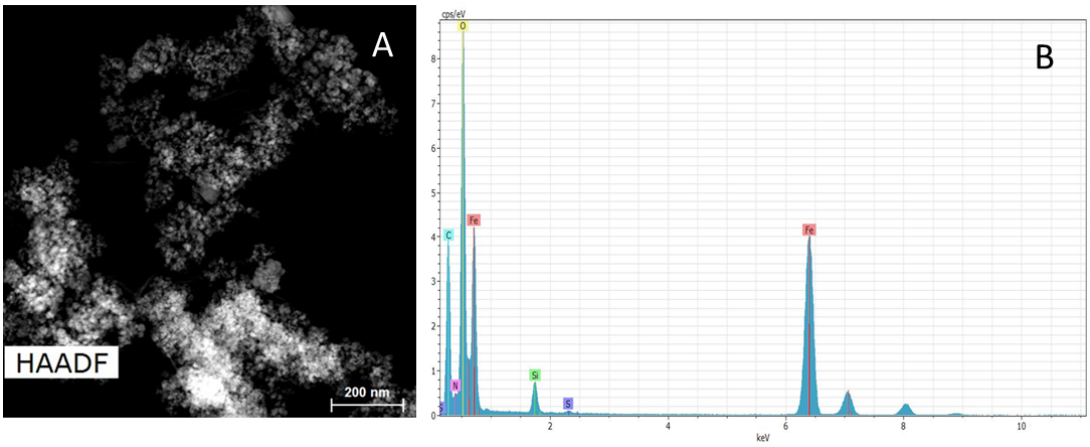

SM3. SEM images (A) DPTH-MNP-GO scale 200 nm and (B) spectrum of DPTH@MGO.

Table SM 4

Analysis of DPTH@MGO SEM spectrum.

Element	[% normalized weight]
Fe	37.661
O	29.028
C	28.899
Si	2.538
N	1.629
S	0.244

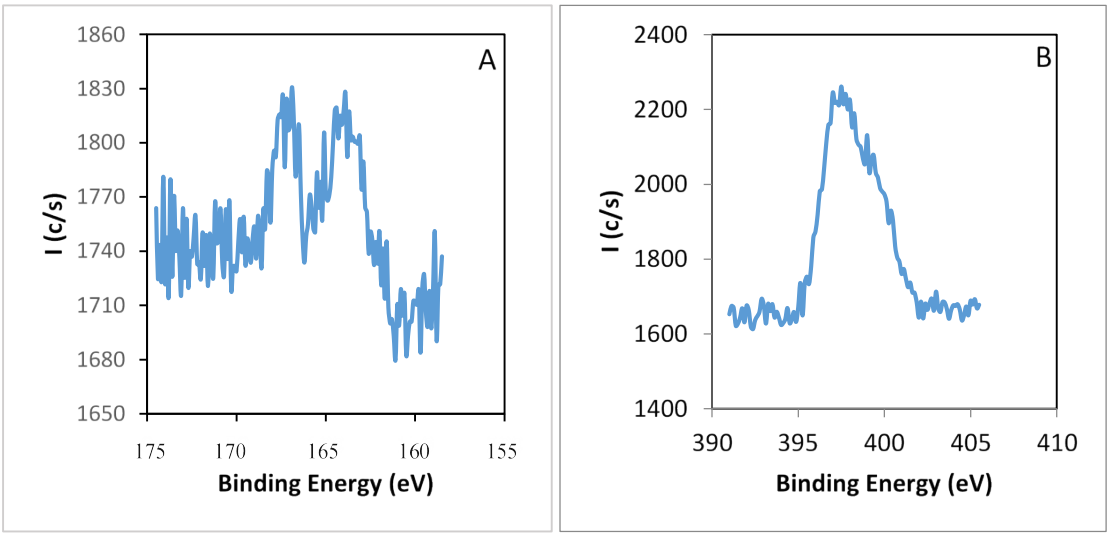

Figure SM 5. XPS spectra (A) S region (B) N region.

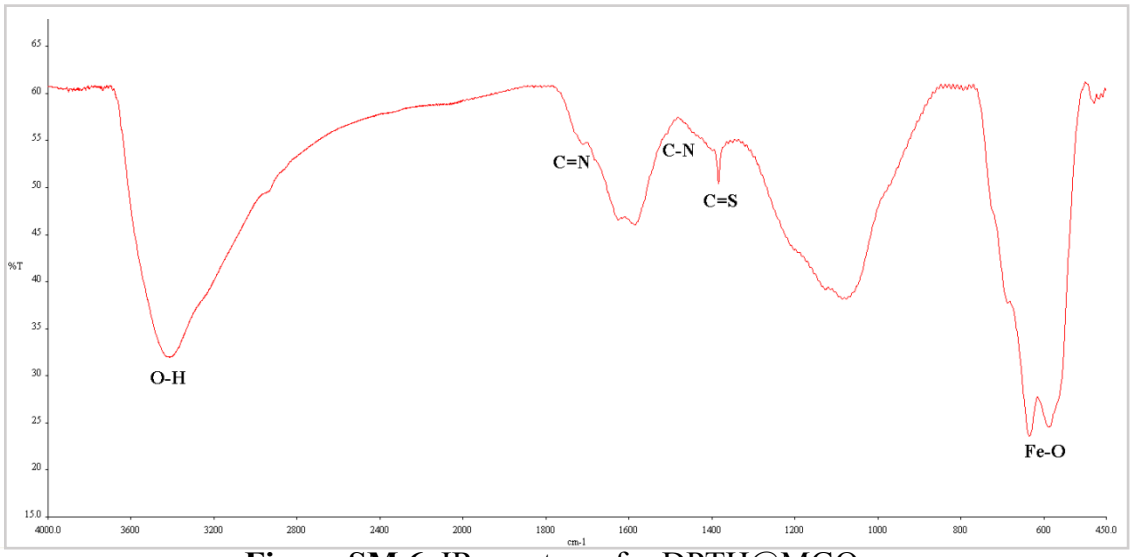

Figure SM 6. IR spectrum for DPTH@MGO.

Table SM 7

Adsorption capacity for DPTH@MGO

Element	DPTH@MGO adsorption capacity (mg g^{-1}) pH 8	DPTH@MGO adsorption capacity (mg g^{-1}) pH 5
Pb	0.65	0.57
Co	0.52	0.52
Zn	0.32	0.15
Cr	0.57	0.55
Ni	0.27	0.37
Cu	0.00	0.00
Cd	0.00	0.00
As	1.22	0.77
Sb	7.66	8.07
Hg	5.18	5.82
Ag	9.75	9.72
Au	9.10	9.25
Pd	6.37	6.50
Ir	0.00	7.42
Pt	5.07	4.50
Os	7.95	6.42

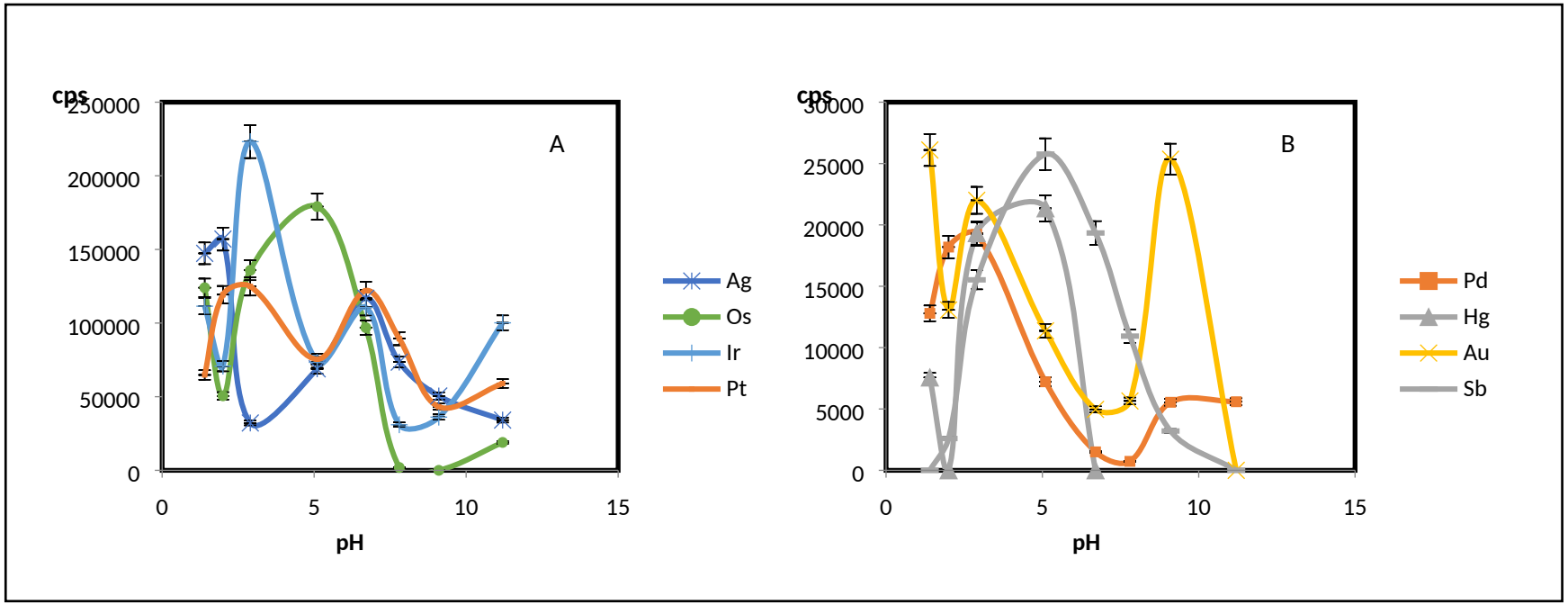

Figure SM 8. Influence of pH on the preconcentration of Ag, Os, Ir and Pt (A); Pd, Hg, Au and Sb (B)